Results in Physics 7 (2017) 16–20

Contents lists available at ScienceDirect

Results in Physics

journal homepage: www.journals.elsevier.com/results-in-physics

Thermally activated flux flow in superconducting epitaxial $FeSe_{0.6}Te_{0.4}$ thin film

D. Ahmad [a], W.J Choi [a], Y.I. Seo [a], Sehun Seo [b], Sanghan Lee [b], Yong Seung Kwon [a,*]

[a] Department of Emerging Materials Science, DGIST, Daegu 42988, Republic of Korea
[b] School of Materials Science and Engineering, GIST, Gwangju 81005, Republic of Korea

ARTICLE INFO

Article history:
Received 23 August 2016
Received in revised form 23 November 2016
Accepted 24 November 2016
Available online 29 November 2016

Keywords:
Thermally activated flus flow
Apparent activation energy
$FeSe_{0.6}Te_{0.4}$ thin film

ABSTRACT

The thermally activated flux flow effect has been studied in epitaxial $FeSe_{0.6}Te_{0.4}$ thin film grown by a PLD method through the electrical resistivity measurement under various magnetic fields for B//c and B//ab. The results showed that the thermally activated flux flow effect is well described by the nonlinear temperature-dependent activation energy. The evaluated apparent activation energy $U_0(B)$ is one order larger than the reported results and showed the double-linearity in both magnetic field directions. Furthermore, the $FeSe_{0.6}Te_{0.4}$ thin film shows the anisotropy of 5.6 near T_c and 2D-like superconducting behavior in thermally activated flux flow region. In addition, the vortex glass transition and the temperature dependence of the high critical fields were determined.

Introduction

The recent discovery of the iron-pnictides superconductor [1], has lead a new direction for the condensed matter physicists for investigating the superconducting phenomena and comparison with other high temperature superconductors. Principally, iron based superconductor can be divided in two classes: the chalcogenides such as FeTe and FeSe and the pnictides [2–6]. In analogy with other high temperature superconductors (HTS), the superconducting state emerges in iron-based superconductors as a competing phenomenon with an antiferromagnetic phase. In case of the FeSe compound, superconductivity is observed in PbO-type structure and its crystal structure is composed of a stack of superconducting Fe_2Se_2 layers along the c-axis [2]. Furthermore, the FeSe system is taken as a key compound in order to explore the mechanism of high temperature superconductivity. The T_c of generic FeSe is as low as 8 K, however it has been reported that the T_c can be substantially enhanced up to 15 K by partial substitution of Se with Te [7,8]. However, enhanced T_c of ~37 K was achieved by the application of hydrostatic pressures [9,10]. Furthermore, in thin films of $FeSe_{1-x}Te_x$ the T_c is enhanced up to 21 K with $x = 0.6$ due to the influence of strain effects induced by the lattice mismatch between the film and substrate [11] Recently, highest T_c of 65 K has recently been reported for monolayer FeSe film [12].

It has been now well established fact that the thermal fluctuations in high temperature superconductors are due to their high T_c, small coherence length, and large anisotropy which is resulted into broadening of the superconducting transition as applied magnetic field is increased [13]. Similarly, iron-based superconductors also show high T_c and short coherence length [14]. However, they exhibit nearly isotropic superconductivity which is a major difference in comparison with other HTS superconductors [12–16]. For instance, in iron based superconductors the thermal fluctuations of vortices can result into thermally activated flux flow (TAFF), which causes the resistive transition curve to shift to lower temperatures and is broadened as the field increases. For example, in case of $REFeAsO_{1-x}F_x$ (RE: rare earth element) [17,18], similar broadening of transition with increasing field was observed which was reported for $YBa_2Cu_3O_{7-\delta}$ (YBCO) [19]. On the other hand, in the case of Ba-122 the thermal fluctuations are negligible as the resistive transition curves shift to low temperatures without showing broadness as the field is increased [20].

In this paper we have investigated the thermally activated flux flow (TAFF) behavior due to the intrinsic and extrinsic pinning effects for nearly optimally doped $FeSe_{0.6}Te_{0.4}$ ($T_c \sim 21$ K) thin film under magnetic field up to 11 T by using the conventional Arrhenius relation and modified TAFF model. It has been shown that the Arrhenius curve slopes are directly related to, but not equal to, the activation energies of $FeSe_{0.6}Te_{0.4}$ thin film. It was also found that $FeSe_{0.6}Te_{0.4}$ thin film can be regarded as 2D-like system, which is dependent on the magnetic field direction in the TAFF region.

* Corresponding author.
E-mail address: yskwon@dgist.ac.kr (Y.S. Kwon).

http://dx.doi.org/10.1016/j.rinp.2016.11.054
2211-3797/

Experimental details

The $FeSe_{0.6}Te_{0.4}$ thin film with 110 nm width was grown on 001 oriented CaF_2 substrates by Pulsed laser deposition (PLD) with a KrF excimer laser (Coherent COMPEX PRO 205F, wavelength: 248 nm). During the growth process, the pressure was maintained below 2×10^{-6} Torr, while the base pressure was 3×10^{-7} Torr. The substrate temperature, laser energy density, repetition rate, and the distance between substrate and target were 400 °C, 3 J/cm^2, 3 Hz, and 4 cm, respectively. The $FeSe_{0.6}Te_{0.4}$ bulk target used for PLD was prepared by the induction melting method for reacting of Fe, Se, and Te small chips at 700 °C. The nominal compositions of FST target was $Fe_{0.94}Se_{0.45}Te_{0.55}$. The sample was characterized by X-ray diffraction (XRD) using Cu Kα radiation source. We found the diffracted peaks of (00*l*), from which the c-lattice constant was evaluated to be 5.858 Å. The temperature dependence of the resistivity was measured down to 2 K in a magnetic field up to 11 T with a standard four-probe method using an Oxford superconducting magnetic system with an interval of 0.1 K. Thin Au-lead wires were attached to the sample with pressing a small indium chip for the sake of removing the contact resistance. The electrical resistivity measurements were performed with constant current with the film size of 5 mm (length) × 1 mm (width) × 110 nm (thickness) and the weak current density below 1 A/cm^2, which shows the ohmic response.

Results and discussion

Fig. 1(a) and (b) show the temperature dependence of the electrical resistivity near the superconducting transition T_c region at B = 0, 1, 2, 3, 5, 7, 9 and 11 T for B//c and B//ab. The zero-field T_c is not very sharp with $\Delta T_c \sim 1.3$ as the T_c (onset) = 21.0 K and the T_c (zero) = 19.7 K, which is similar to the reported result of $FeSe_{0.5}Te_{0.5}$ thin films [16]. With increasing magnetic fields, the T_c shifts to lower temperature observed in both magnetic field directions however it is weaker for B//ab: a zero resistivity state shifts down to 16.0 K for B//c and 18.2 K for B//ab at B = 11 T. From Fig. 1, the B_{c2} and the B_{irr} were determined by the usual criterion of 90 and 10% of the normal state resistivity, respectively [20,21]. The result for the $B_{c2}(T)$ is shown in Fig. 2 and $B_{c2}(T)$ increases with very steep slope as temperature decreases but slopes are less steep in case of the $B_{irr}(T)$ for the both field directions. The fitted slopes for $B_{c2}(T)$ and $B_{irr}(T)$ below B = 2 T are 12.4 T/ K and 3.7 T/K for B//c and 45.7 T/K and 12.2 T/K for B//ab, respectively, which are approximately in agreement with previous reported results [11]. The anisotropy determined from $B_{irr}(T)$ curves for both field directions steeply increases from ~ 2.5–5 when the temperature is very close to T_c as shown in the inset of Fig. 2. The anisotropy of ~ 2.5 well below T_c is similar to the reported results in the Fe(Se,Te) film [11]. Within the weak coupling BCS theory [22] and by using the initial slope of B_{c2}-line and B_{irr}-line, the higher critical magnetic field $B^c_{c2}(0)$ was evaluated to be 180 T and 54 T for B//c and $B^{ab}_{c2}(0) = 664$ T and 176 T for B//ab from $B_{c2}(0) = -0.693 T_c (dB_{c2}/dT|_{T_c})$. On the other hand, the Pauli paramagnetic limiting field for weakly coupled BCS superconductors [23] is given by $\mu_0 B_p(0) = 1.84 T_c = 37.4$ T, which is considerably smaller than the higher critical field in both magnetic field directions. This implies that the orbital effect may be the dominant pair-breaking mechanism for both magnetic field directions. The anisotropy factor $\gamma(0) = B^{ab}_{c2}(0)/B^c_{c2}(0)$ was determined to be 3.7.

From the slopes $B'^c_{c2} = |dB^c_{c2}/dT|$ and $B'^{ab}_{c2} = |dB^{ab}_{c2}/dT|$ the GL coherence lengths, $\xi_{ab,0}$ and $\xi_{c,0}$, are evaluated using the relation $B'^c_{c2} = \phi_0/2\pi\xi^2_{ab,0}T_c$ and $B'^{ab}_{c2} = \phi_0/2\pi\xi_{ab,0}\xi_{c,0}T_c$ with B_{c2} is used on the determining the slope. The estimated in-plane and c-axis GL coherence lengths are $\xi_{ab,0} = 1.126$ nm and $\xi_{c,0} = 0.305$ nm, respectively. The anisotropy factor estimated from the coherence length, $\gamma(0) = \frac{\xi_{ab,0}}{\xi_{c,0}}$, is 3.8 which is equal to estimated value from the higher critical field. The $\xi_{c,0}$ is about 2 times smaller than the distance between the FeSe-layers indicating the 2D-like nature of the sample although the anisotropy is smaller than that of cuprates. Fig. 3(a) and (b) show the temperature dependence of

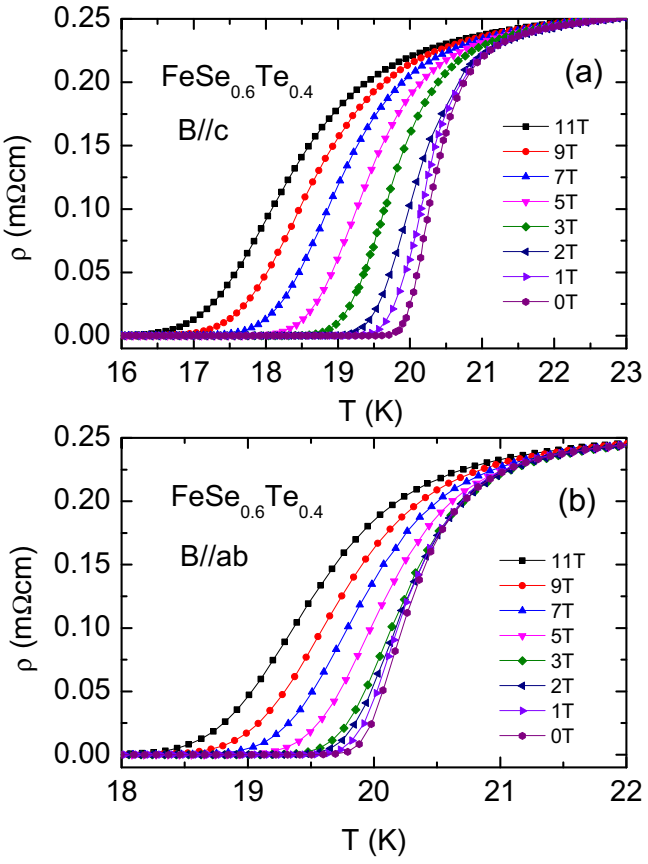

Fig. 1. The temperature dependence of electrical resistivity near T_c region for B//c (a) and B//ab (b) in $FeSe_{0.6}Te_{0.4}$ thin film.

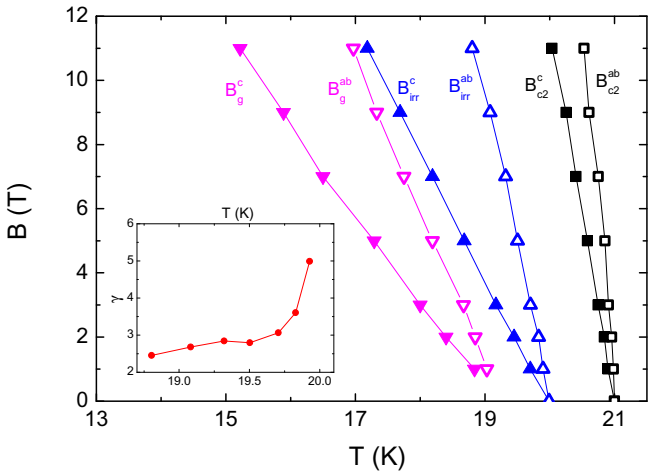

Fig. 2. Static vortex phase diagram for B//c and B//ab in in $FeSe_{0.6}Te_{0.4}$ thin film. The upper critical fields of B_{c2} and B_{irr} as well as the vortex glass temperature are presented. Inset shows the anisotropy ratio from the irreversible magnetic field defined by $\gamma = B^{ab}_{irr}/B^c_{irr}$.

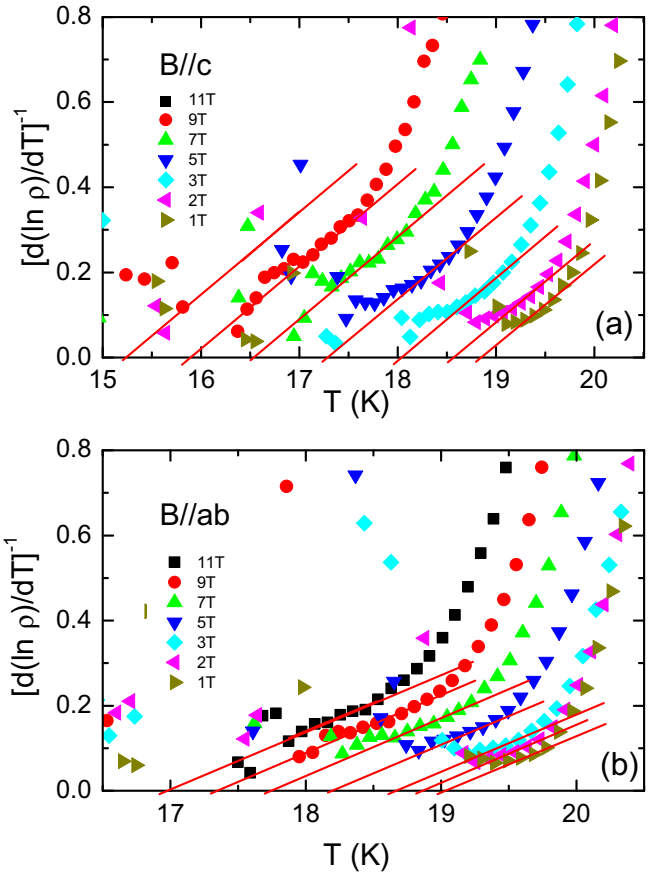

Fig. 3. The temperature dependence of for B//c (a) and B//ab (b) in the $FeSe_{0.6}Te_{0.4}$ thin film, red-colored solid lines represent the best linear fits. (For interpretation of the references to color in this figure legend, the reader is referred to the web version of this article.)

$\left[d\left(\ln\frac{\rho}{dT}\right)\right]^{-1}$ at $B = 1$, 2, 3, 5, 7, 9, 11 T for B//c and B//ab in $FeSe_{0.6}Te_{0.4}$ thin film, respectively, which is used to analyze the vortex glass transition boundary. According to the vortex-glass theory [24], the resistivity follows the relation $\rho \sim (T - T_g)^s$ in the very vicinity of the vortex-glass temperature T_g, where s is the exponent related to the vortex-glass correlation. Using the relation $[d(\ln \rho/dT)]^{-1} \propto (T - T_g)/s$, T_g and s can be extracted from the intercept and slope in $[d(\ln \rho/dT)]^{-1}$vs.T plot. As shown in Fig. 3, the resistivity can be well described by the vortex-glass model with $s = 5.0 \pm 0.3$ for B//c and 7.0 ± 0.3 for B//ab. The s-values are somewhat larger than $s = 2.2$–2.3 determined in $FeTe_{0.6}Se_{0.4}$ and LiFeAs single crystals [25,26] but are similar to the result for YBCO thin film with strong pinning [19]. The estimated vortex glass temperature line is shown in Fig. 2.

In the mixed dissipative state, the electrical resistivity decreases exponentially with a tail in lower-side temperature region than superconducting transition temperature due to the thermally activated flux flow. According to the thermally activated flux flow theory [27,28], the resistivity is theoretically expressed as

$$\rho = (2\nu_0 LB/J)\exp(-J_{c0}BVL/T)\sinh(JBVL/T), \quad (1)$$

where ν_0 is an attempt frequency for a flux bundle hopping, L is the hopping distance, B the magnetic induction, J the applied current density, J_{c0} the critical current density in the absence of flux creep, V the bundle volume and T the temperature. If J is small enough so that $JBVL/T \ll 1$, Eq. (1) is simplified to

$$\rho = (2\rho_c U/T)\exp(-U/T) \quad (2)$$

where $U = J_{c0}BVL$, called as the thermally activated energy (TAE) and $\rho_c = \nu_0 LB/J_{c0}$. The coefficient of Eq. (2) is temperature- and magnetic-field-dependent. In some cuprates and FeAs-based superconductors, however, it is assumed that the coefficient $2\rho_c U/T$ is temperature-independent constant of ρ_{0f}. Under this assumption, we can obtain the relation $U(T,B) = U_0(1-t)$ and $\ln\rho(T,B) = \ln\rho_0(B) - U_0(B)/T$, where $t = T/T_c$, T_c is superconducting transition temperature, $\ln\rho_0(B) = \ln\rho_{0f} + U_0(B)/T_c$ and $U_0(B)$ is the apparent activation energy. From this relation, $\ln\rho$ is linear to $1/T$, which is called an Arrhenius relation. In order to identify the Arrhenius relation, we plot the relation of $\ln\rho$ vs. $1/T$ in Fig. 4. This result is different from the result for $FeSe_{0.5}Te_{0.5}$ thin film [21] and FeSe single crystal [29] which showed the Arrhenius relation [21]. This difference may be due to the difference of measurement resolution: In our measurement the resistivity was measured from $\sim 10^{-8}$ Ωcm, while in the previous reports the resistivity was measured from $\sim 10^{-7}$ Ωcm [21,29] (This indicates that our measurement was performed from the temperature close to superconducting transition temperature). In order to identify the temperature dependence of U_0, we obtained the temperature dependence of the activation energy from the Arrhenius relation, $U_0 = -\partial\ln\rho(T,B)/\partial(1/T)$, which is plotted in Fig. 5 showing that

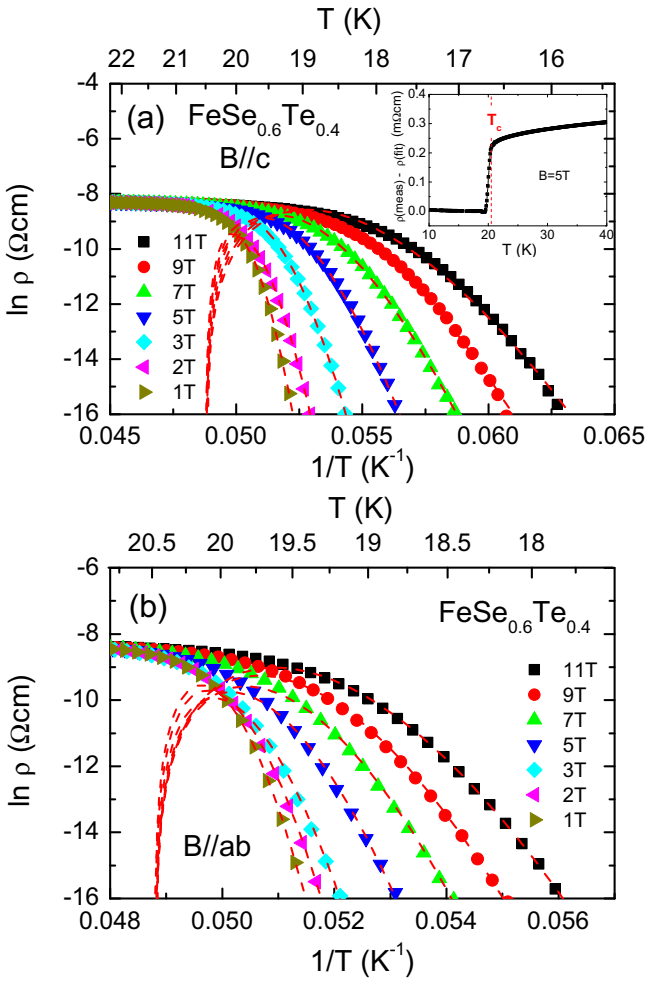

Fig. 4. The $\ln\rho(T)$ vs. $1/T$ plot for B//c (a) and $\rho_0(B)$ for B//ab (b) in $FeSe_{0.6}Te_{0.4}$ thin film. The red-colored dashed line is obtained by the modified method considering nonlinear temperature-dependent activation energy. Inset of figure (a) shows the electrical resistivity subtracting the fitted data of TAFF analysis from the measuring resistivity data at $B = 5$ T. The red-colored dashed line means the transition temperature $T_c = 20.5$ K. (For interpretation of the references to color in this figure legend, the reader is referred to the web version of this article.)

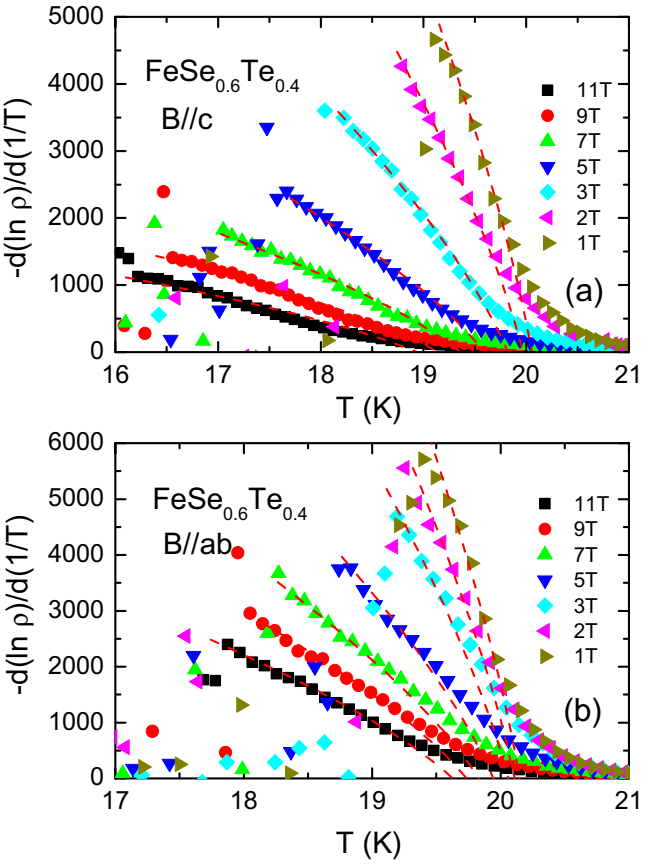

Fig. 5. The temperature dependence of the activation energy, $-\partial \ln \rho(T,B)/\partial(1/T)$, for B//c (a) and B//ab (b) in $FeSe_{0.6}Te_{0.4}$ thin film. Red-colored dashed lines are regression curves with the fitting parameters $U_0(B)$ and $\rho_c(B)$ determined from the modified analytic method. (For interpretation of the references to color in this figure legend, the reader is referred to the web version of this article.)

the activation energy increases with decreasing temperature. It can be noted that the increase is more rapid with decreasing magnetic fields. Similar behavior was also observed in cuprates and iron-based superconductors [18,25,30–32]. Therefore, analysis of the activation energy cannot be performed by the simple Arrhenius relation in this material. In order to solve this contradiction, the effect of temperature-dependent coefficient and the temperature-nonlinear relation of $U(T,B)$ must be considered, which is called as a modified TAFF method suggested by Zhang et al. [18]. By applying their suggestion to Eq. (2) with $U = U_0(1-t)^q$, it can be derived that

$$\ln \rho = \ln(2\rho_0 U_0) + q\ln(1-t) - \ln T - U_0(1-t)^q/T \quad (3)$$

and

$$-\partial \ln \rho/\partial(1/T) = [U_0(1-t)^q - T][1 + qt/(1-t)], \quad (4)$$

where q has a value in the range from 0.5 to 2. There are four free parameters ρ_0, U_0, q and T_c in Eq. (3) but three free parameters U_0, q and T_c in Eq. (4). To obtain more precise values for parameters in the regression process, we first tried the data regression using Eq. (4) to determine three parameters U_0, q and T_c and then again the data regression for Eq. (3) to determine value of the parameter ρ_0, in which we used the value of the three parameters obtained from the first process as initial values in the last process. The red-colored dashed lines in Fig. 4(a)-(b) and Fig. 5(a)-(b) are regression curves with the regression parameters $U_0(B)$ and $\rho_c(B)$ using Eq. (3) for B//c and B//ab, respectively. The regression is well fitted the measured data in wide temperature regions below the $\sim T_c$. We, for instance, plotted the electrical resistivity subtracting the regression data of TAFF analysis from the measuring resistivity data at $B = 5$ T in the inset of Fig. 4. As shown the inset, the subtracted resistivity do not show the exponential increase in lower-side temperature region than T_c due to TAFF and slowly increases above T_c due to the electron-phonon scattering. The round effect downward was observed just above T_c, which is due to the thermal fluctuation of Cooper-pairs. In this regression we found that the energy relation of $U(T,B) = U_0(B)(1-t)^q$ with $q = 2$ leads to a good agreement with the experimental data, where $t = T/T_c$ and $T_c = 20.5$ K in both B//c and B//ab, which is similar to the results of $Fe(Te_{1-x}S_x)$ and $SmFeAs_{0.9}F_{0.1}$ [18,30], which generally show 2-dimensional behavior with a similar scaling. Therefore, $FeSe_{0.6}Te_{0.4}$ superconducting thin film has very small anisotropy comparing with cuprates but it is regarded as a 2D-like system in the TAFF region, which is consistent with the coherence length result mentioned before. The parameter of $\rho_0(B)$ is slowly increasing with magnetic fields in both magnetic field directions, which is drawn in the inset of Fig. 6.

As shown in Fig. 6, the values of U_0 determined from this method are about 4.3×10^4 and 6.8×10^4 K at $B = 1$ T for B//c and B//ab, respectively, which are decreased down to 3.3×10^3 and 1.0×10^4 K with increasing magnetic fields. These values of U_0 are one order larger than the values reported in some FeAs-based superconductors but are similar to $SmFeAsO_{0.9}F_{0.1}$, $Ba_{0.72}K_{0.28}Fe_2As_2$ and cuprate thin films [18–20]. Especially, in undoped FeSe single crystal the U_0 values are isotropic and are 200–300 times smaller than our values for the optimal doped sample [29]. The observed anisotropy of U_0 in our sample which is optimally doped indicates that the difference of U_0 between undoped and optimally doped samples is not due to the impurity effect but due to the change of intrinsic superconducting properties. Note that the anisotropy should not be observed if the increase of U_0 in optimally doped sample compared with the undoped sample is due to only impurity effect. Moreover, the value of U_0 in our case are 15 and 30 times larger than those of nearly optimally doped $FeSe_{0.5}Te_{0.5}$ thin film [21] and $FeTe_{0.6}Se_{0.4}$ single crystal [33], respectively. In the $FeSe_{0.5}Te_{0.5}$ thin film, the U_0 was determined from the Arrhenius relation and seems to be estimated smaller. In the $FeTe_{0.6}Se_{0.4}$ single crystal the difference with our case may arise from the difference of T_c and measurement resolution. Note that the apparent activation energy as shown in Fig. 3 rapidly decreases with increasing temperature in low magnetic fields

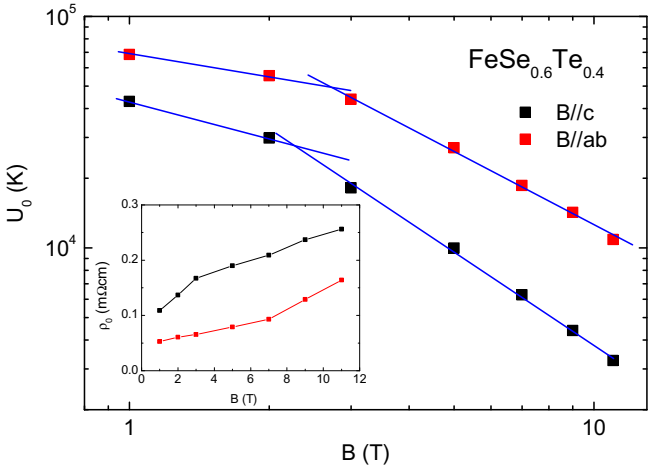

Fig. 6. The apparent activation energy $U_0(B)$ determined by the modified analytic method for B//c and B//ab in $FeSe_{0.6}Te_{0.4}$ thin film. Solid lines show the best linear fits. Inset shows the magnetic field dependence of determined by the modified analytic method.

and the determined apparent activation energy becomes considerably smaller if it is evaluated from a higher temperature region.

The determined values of U_0 in B//ab are 60–230% larger than those in B//c, which indicates that the intrinsic pinning between the FeSe layers is dominant for B//ab and is stronger than the extrinsic pinning due to stacking faults and defects dominant for B//c as mentioned just above. However, the large U_0 values are decreased rapidly with increasing magnetic field in both field directions. The magnetic field dependence of U_0 shows a double-linearity in log-log scale, indicating that it follows a power law of $U_0(B) \sim B^{-\alpha}$ with $\alpha = 0.52$ in $B < 2$ T and $\alpha = 1.32$ in $B > 3$ T in case of B//c, and $\alpha = 0.3$ in $B < 2$ T and$\alpha = 1.07$ in $B > 3$ T in case of B//ab. A similar behavior was also reported in Fe(Se,Te) thin film [17,29] and single crystal [26], cuprate [19] and other FeAs-based superconductors [17], where the double-linearity was explained by the transition from a single-vortex pinning to a collective-vortex pinning. In the state of the single-vortex pinning occurring in low magnetic fields, the overlap of vortex is negligible and the field dependence is weak. Meanwhile, on increasing the magnetic field up to a certain amount which results into significant overlap of vortices, the pinning energy begins to be distinctively suppressed and the field dependence is strong. Therefore, in $FeSe_{0.6}Te_{0.4}$ thin film the crossover from strong to weak pinning seems to happen at around 2–3 T in both magnetic field directions.

Conclusion

Epitaxial $FeSe_{0.6}Te_{0.4}$ thin film grown by a PLD method was measured electrical resistivity under various magnetic fields at B//c and B//ab for studying the thermally activated flux flow. As a result, the broadening near the superconducting transition in the resistivity under magnetic fields was observed in the both magnetic field directions due to the thermally activated flux flow with the evidence of strong activation energy. The magnetic field dependence of the activation energy shows double-linearity with boundary of 2–3 T. Since the considerably large activation energy is observed in B//ab, comparing with B//c, we conclude that the intrinsic pinning between the FeSe layers is dominant and is stronger than the extrinsic pinning due to stacking faults and defects.

Acknowledgements

This work was supported by the NRF grant funded by the Ministry of Science, ICT and Future Planning (2015M2B2A9028507, 2016R1A2B4012672 and 2012K1A4A3053565).

References

[1] Kamihara Y, Watanabe T, Hirano M, Hosono H. J. Am. Chem. Soc. 2008;130:3296.
[2] Hsu F-C, Luo J-Y, Yeh L-W, Chen T-K, Huang T-W, Wu PM, et al. Proc. Natl. Acad. Sci. U.S.A. 2008;105:14262.
[3] Tapp JH, Tang Z, Lv B, Sasmal K, Lorenz B, Chu PC, Guloy AM. Phys. Rev. B 2008;78:060505.
[4] Rotter M, Tegel M, Johrendt D. Phys. Rev. Lett. 2008;101:107006.
[5] Zhu X, Han F, Mu G, Zeng B, Cheng P, Shen B, Wen HH. Phys. Rev. B 2009;79:024516.
[6] Ogino H, Machida K, Yamamoto A, Kishio K, Shimoyama J, Tohei T, Ikuhara Y. Supercond. Sci. Technol. 2010;23:115005.
[7] Yeh K-W, Huang T-W, Huang Y-L, Chen T-K, Hsu F-C, Wu PM, et al. Europhys. Lett. 2008;84:37002.
[8] Fang MH, Pham HM, Qian B, Liu TJ, Vehstedt EK, Liu Y, Spinu L, Mao ZQ. Phys. Rev. B 2008;78:224503.
[9] Medvedev S, McQueen TM, Troyan IA, Palasyuk T, Eremets MI, Cava RJ, Naghavi S, Casper F, Ksenofontov V, Wortmann G, Felser C. Nat. Mater. 2009;8:630.
[10] Margadonna S, Takabayashi Y, Ohishi Y, Mizuguchi Y, Takano Y, Kagayama T, Nakagawa T, Takata M, Prassides K. Phys. Rev. B 2009;80:064506.
[11] Bellingeri E, Kawale S, Caglieris F, Braccini V, Lamura G, Pellegrino L, Sala A, Putti M, Ferdeghini C, Jost A, Zeitler U, Tarantini C, Jaroszynski J. Supercond. Sci. Technol. 2014;27:044007.
[12] He SL, He JF, Zhang WH, Zhao L, Liu DF, Liu X, Mou DX, Ou Y-B, Wang Q-Y, Li Z, Wang LL, Peng YY, Liu Y, Chen CY, Yu L, Liu GD, Dong XL, Zhang J, Chen CT, Xu ZY, Chen X, Ma XC, Xue QK, Zhou XJ. Nat. Mater. 2013;12:605.
[13] Mun MO, Lee SI, Lee WC. Phys. Rev. B 1997;56:14688.
[14] Liu SL, Gong L, Gang B, Wang H, Li B. Supercond. Sci. Technol. 2011;24:078005.
[15] Kim DH, Gray KE, Trochet MD. Phys. Rev. B 1997;45:10801.
[16] Pallecchi I, Fanciulli C, Tropeano M, Palenzona A, Ferretti M, Malagoli A, Martinelli A, Sheikin I. Phys. Rev. B 2009;79:104515.
[17] Jaroszynski J, Hunte F, Balicas L, Jo Youn-jung, Raičević I, Gurevich A, Larbalestier DC, Balakirev FF, Fang L, Cheng P, Jia Y, Wen Hh. Phys. Rev. B 2008;78:174523.
[18] Zhang YZ, Ren ZA, Zhao ZX. Supercond. Sci. Technol. 2009;22:065012.
[19] Zhang YZ, Wen HH, Wang Z. Phy. Rev B 2006;74:144521.
[20] Wang Xiao-Lin, Ghorbani SR, Lee Sung-Ik, Dou SX, Lin CT, Johansen TH. Phys. Rev. B 2010;82:024525.
[21] Shahbazi M, Wang XL, Ghorbani SR, Dou SX, Choi KY. App. Phys. Lett 2012;100:102601.
[22] Werthamer NR, Helfant E, Hohenberg PC. Phys. Rev. B 1966;147:295.
[23] Clogston AM. Phys. Rev. Lett. 1962;9:266.
[24] Fisher MPA. Phys. Rev. Lett. 1989;62:1415.
[25] Song YJ, Kang BW, Rhee JS, Kwon YS. EPL 2012;97:47003.
[26] Shahbazi M, Wang XL, Ghorbani SR, Dou SX, Lin CT. Physica C 2015;519:60.
[27] Blatter G, Feigel'man MV, Geshkenbein VB, Larkin AI, Vinokur VM. Rev. Mod. Phys. 1994;66:1125.
[28] Palstra TTM, Batlogg B, Schneemeyer LF, Waszczak JV. Phys. Rev. Lett. 1998;61:1662.
[29] Lei, H, Hu, R, Petrovic, C. Phys Rev B 84: 014520.
[30] Lei H, Hu R, Choi ES, Petrovic C. Phys. Rev. B 2010;82:134525.
[31] Shahbazi M, Wang XL, Shekhar C, Srivastava ON, Lin ZW, Zhu JG, Dou SX. J. App. Phys. 2011;109:07E162.
[32] Geshkenbein VB, Feigel'man MV, Larkin AI, Vinokur VM. Physica C 1989;162:239.
[33] Chang HH, Luo JY, Wu CT, Hsu FC, Huang TW, Wu PM, Wu MK, Wang MJ. Supercond. Sci. Technol. 2011;24:105011.